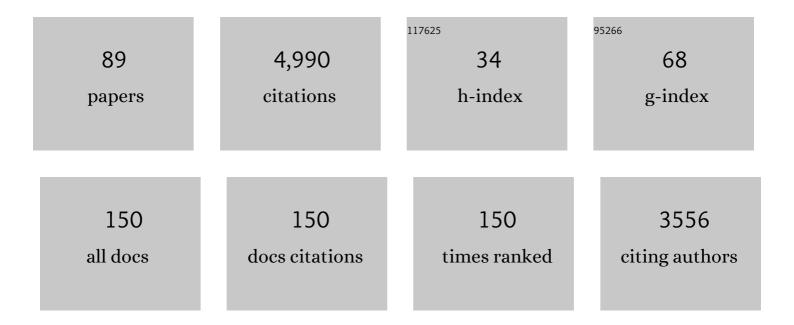
List of Publications by Year in descending order

Source: https://exaly.com/author-pdf/2513347/publications.pdf Version: 2024-02-01



RODIS LD KALIS

#	Article	IF	CITATIONS
1	Aftershocks driven by a high-pressure CO2 source at depth. Nature, 2004, 427, 724-727.	27.8	714
2	A benchmark comparison of spontaneous subduction models—Towards a free surface. Physics of the Earth and Planetary Interiors, 2008, 171, 198-223.	1.9	361
3	Delamination and recycling of Archaean crust caused by gravitational instabilities. Nature Geoscience, 2014, 7, 47-52.	12.9	358
4	A comparison of numerical surface topography calculations in geodynamic modelling: an evaluation of the †sticky air' method. Geophysical Journal International, 2012, 189, 38-54.	2.4	301
5	Numerical modelling of magma dynamics coupled to tectonic deformation of lithosphere and crust. Geophysical Journal International, 2013, 195, 1406-1442.	2.4	152
6	A free plate surface and weak oceanic crust produce singleâ€sided subduction on Earth. Geophysical Research Letters, 2012, 39, .	4.0	147
7	Initiation of localized shear zones in viscoelastoplastic rocks. Journal of Geophysical Research, 2006, 111, .	3.3	141
8	A stabilization algorithm for geodynamic numerical simulations with a free surface. Physics of the Earth and Planetary Interiors, 2010, 181, 12-20.	1.9	140
9	Numerical investigation of deformation mechanics in foldâ€andâ€thrust belts: Influence of rheology of single and multiple décollements. Tectonics, 2012, 31, .	2.8	124
10	Shear heating induced lithospheric-scale localization: Does it result in subduction?. Earth and Planetary Science Letters, 2012, 359-360, 1-13.	4.4	119
11	Factors that control the angle of shear bands in geodynamic numerical models of brittle deformation. Tectonophysics, 2010, 484, 36-47.	2.2	109
12	Comparison of Eulerian and Lagrangian numerical techniques for the Stokes equations in the presence of strongly varying viscosity. Physics of the Earth and Planetary Interiors, 2008, 171, 92-111.	1.9	96
13	Effect of mineral phase transitions on sedimentary basin subsidence and uplift. Earth and Planetary Science Letters, 2005, 233, 213-228.	4.4	93
14	Mixing instabilities during shearing of metals. Nature Communications, 2017, 8, 1611.	12.8	92
15	From passive continental margin to mountain belt: Insights from analytical and numerical models and application to Taiwan. Physics of the Earth and Planetary Interiors, 2008, 171, 235-251.	1.9	89
16	Effects of elasticity on the Rayleigh-Taylor instability: implications for large-scale geodynamics. Geophysical Journal International, 2007, 168, 843-862.	2.4	88
17	The numerical sandbox: comparison of model results for a shortening and an extension experiment. Geological Society Special Publication, 2006, 253, 29-64.	1.3	84
18	Benchmarking numerical models of brittle thrust wedges. Journal of Structural Geology, 2016, 92, 140-177.	2.3	81

#	Article	IF	CITATIONS
19	3D finite amplitude folding: Implications for stress evolution during crustal and lithospheric deformation. Geophysical Research Letters, 2006, 33, .	4.0	72
20	Intrusion of granitic magma into the continental crust facilitated by magma pulsing and dikeâ€diapir interactions: Numerical simulations. Tectonics, 2016, 35, 1575-1594.	2.8	69
21	Dynamic constraints on the crustal-scale rheology of the Zagros fold belt, Iran. Geology, 2011, 39, 815-818.	4.4	66
22	Intermediate-depth earthquake generation and shear zone formation caused by grain size reduction and shear heating. Geology, 2015, 43, 791-794.	4.4	66
23	Geodynamic inversion to constrain the non-linear rheology of the lithosphere. Geophysical Journal International, 2015, 202, 1289-1316.	2.4	64
24	Thermomechanical modeling of slab eduction. Journal of Geophysical Research, 2012, 117, .	3.3	58
25	Selfâ€consistent subduction initiation induced by mantle flow. Terra Nova, 2015, 27, 130-138.	2.1	57
26	Constraining effective rheology through parallel joint geodynamic inversion. Tectonophysics, 2014, 631, 197-211.	2.2	56
27	Forward and reverse modeling of the three-dimensional viscous Rayleigh-Taylor instability. Geophysical Research Letters, 2001, 28, 1095-1098.	4.0	54
28	Development of topography in 3â€D continentalâ€collision models. Geochemistry, Geophysics, Geosystems, 2015, 16, 1378-1400.	2.5	52
29	Subduction metamorphism in the Himalayan ultrahigh-pressure Tso Morari massif: An integrated geodynamic and petrological modelling approach. Earth and Planetary Science Letters, 2017, 467, 108-119.	4.4	52
30	Stress-strength relationship in the lithosphere during continental collision. Geology, 2009, 37, 775-778.	4.4	50
31	Nonlithostatic pressure during subduction and collision and the formation of (ultra)high-pressure rocks. Geology, 2016, 44, 343-346.	4.4	45
32	On the Quality of Velocity Interpolation Schemes for Marker-in-Cell Method and Staggered Grids. Pure and Applied Geophysics, 2017, 174, 1071-1089.	1.9	44
33	Parameters that control lithosphericâ€scale thermal localization on terrestrial planets. Geophysical Research Letters, 2010, 37, .	4.0	41
34	Potential causes for the nonâ€Newtonian rheology of crystalâ€bearing magmas. Geochemistry, Geophysics, Geosystems, 2011, 12, .	2.5	37
35	Dome structures in collision orogens: Mechanical investigation of the gravity/compression interplay. , 2004, , .		33
36	Comparing thin-sheet models with 3-D multilayer models for continental collision. Geophysical Journal International, 2011, 187, 10-33.	2.4	33

#	Article	IF	CITATIONS
37	Fold interaction and wavelength selection in 3D models of multilayer detachment folding. Tectonophysics, 2014, 632, 199-217.	2.2	32
38	Generation of Earth's Early Continents From a Relatively Cool Archean Mantle. Geochemistry, Geophysics, Geosystems, 2019, 20, 1679-1697.	2.5	31
39	Thermal localization as a potential mechanism to rift cratons. Physics of the Earth and Planetary Interiors, 2011, 186, 125-137.	1.9	26
40	The role of slabs and oceanic plate geometry in the net rotation of the lithosphere, trench motions, and slab return flow. Geochemistry, Geophysics, Geosystems, 2012, 13, .	2.5	26
41	Lithospheric stress-states predicted from long-term tectonic models: Influence of rheology and possible application to Taiwan. Journal of Asian Earth Sciences, 2009, 36, 119-134.	2.3	24
42	Sedimentology of early Pliocene sandstones in the south-western Taiwan foreland: Implications for basin physiography in the early stages of collision. Journal of Asian Earth Sciences, 2011, 40, 52-71.	2.3	24
43	Modeling of wind gap formation and development of sedimentary basins during fold growth: application to the Zagros Fold Belt, Iran. Earth Surface Processes and Landforms, 2016, 41, 1521-1535.	2.5	23
44	Slab-triggered wet upwellings produce large volumes of melt: Insights into the destruction of the North China Craton. Tectonophysics, 2018, 746, 266-279.	2.2	23
45	Subductionâ€Induced Backâ€Arc Extension Versus Farâ€Field Stretching: Contrasting Modes for Continental Marginal Breakâ€Up. Geochemistry, Geophysics, Geosystems, 2021, 22, e2020GC009416.	2.5	23
46	Subduction Polarity Reversal Triggered by Oceanic Plateau Accretion: Implications for Induced Subduction Initiation. Geophysical Research Letters, 2021, 48, e2021GL095299.	4.0	23
47	Indentation as an extrusion mechanism of lower crustal rocks: Insight from analogue and numerical modelling, application to the Eastern Bohemian Massif. Lithos, 2011, 124, 158-168.	1.4	21
48	Plume — Lid interactions during the Archean and implications for the generation of early continental terranes. Gondwana Research, 2020, 88, 150-168.	6.0	21
49	Influences of surface processes on fold growth during 3â€D detachment folding. Geochemistry, Geophysics, Geosystems, 2014, 15, 3281-3303.	2.5	20
50	Discretization Errors in the Hybrid Finite Element Particle-in-cell Method. Pure and Applied Geophysics, 2014, 171, 2165-2184.	1.9	20
51	Influence of surface processes and initial topography on lateral fold growth and fold linkage mode. Tectonics, 2015, 34, 1622-1645.	2.8	20
52	Lower Crustal Rheology Controls the Development of Large Offset Strikeâ€5lip Faults During the Himalayanâ€īibetan Orogeny. Geophysical Research Letters, 2020, 47, e2020GL089435.	4.0	20
53	The effect of rheological approximations in 3-D numerical simulations of subduction and collision. Tectonophysics, 2018, 746, 296-311.	2.2	19
54	Rheological controls on the terrestrial core formation mechanism. Geochemistry, Geophysics, Geosystems, 2009, 10, .	2.5	18

#	Article	IF	CITATIONS
55	Quantifying the impact of mechanical layering and underthrusting on the dynamics of the modern Indiaâ€Asia collisional system with 3â€D numerical models. Journal of Geophysical Research: Solid Earth, 2014, 119, 616-644.	3.4	18
56	The mechanics of continental transforms: An alternative approach with applications to the San Andreas system and the tectonics of California. Earth and Planetary Science Letters, 2008, 274, 380-391.	4.4	17
57	Influence of pre-existing salt diapirs on 3D folding patterns. Tectonophysics, 2014, 637, 354-369.	2.2	17
58	Development of branching brittle and ductile shear zones: A numerical study. Geochemistry, Geophysics, Geosystems, 2017, 18, 2054-2075.	2.5	17
59	Lithospheric stresses in Rayleigh–Bénard convection: effects of a free surface and a viscoelastic Maxwell rheology. Geophysical Journal International, 2015, 203, 2200-2219.	2.4	16
60	Pattern formation in 3-D numerical models of down-built diapirs initiated by a Rayleigh–Taylor instability. Geophysical Journal International, 2015, 202, 1253-1270.	2.4	16
61	Unraveling the Physics of the Yellowstone Magmatic System Using Geodynamic Simulations. Frontiers in Earth Science, 2018, 6, .	1.8	16
62	Direct numerical simulation of two-phase flow: Effective rheology and flow patterns of particle suspensions. Earth and Planetary Science Letters, 2010, 290, 1-12.	4.4	15
63	Strong intracontinental lithospheric deformation in South China: Implications from seismic observations and geodynamic modeling. Journal of Asian Earth Sciences, 2014, 86, 106-116.	2.3	15
64	Effect of pressure and temperature on viscosity of a borosilicate glass. Journal of the American Ceramic Society, 2018, 101, 3936-3946.	3.8	15
65	Pore-scale permeability prediction for Newtonian and non-Newtonian fluids. Solid Earth, 2019, 10, 1717-1731.	2.8	15
66	Insights into the Compositional Evolution of Crustal Magmatic Systems from Coupled Petrological-Geodynamical Models. Journal of Petrology, 2020, 61, .	2.8	13
67	A Multiphysics Approach to Constrain the Dynamics of the Altiplanoâ€Puna Magmatic System. Journal of Geophysical Research: Solid Earth, 2021, 126, e2021JB021725.	3.4	12
68	Slow Geodynamics and Fast Morphotectonics in the Far East Tethys. Geochemistry, Geophysics, Geosystems, 2022, 23, .	2.5	10
69	Dynamic pressure variations in the lower crust caused by localized fluid-induced weakening. Communications Earth & Environment, 2022, 3, .	6.8	10
70	Speculations on the impact of catastrophic subduction initiation on the Earth System. Journal of Geodynamics, 2016, 93, 1-16.	1.6	9
71	Deriving scaling laws in geodynamics using adjoint gradients. Tectonophysics, 2018, 746, 352-363.	2.2	9
72	Inferring rheology and geometry of subsurface structures by adjoint-based inversion of principal stress directions. Geophysical Journal International, 2020, 223, 851-861.	2.4	9

#	Article	IF	CITATIONS
73	Investigating the effects of intersection flow localization in equivalent-continuum-based upscaling of flow in discrete fracture networks. Solid Earth, 2021, 12, 2235-2254.	2.8	9
74	Self-replicating subduction zone initiation by polarity reversal. Communications Earth & Environment, 2022, 3, .	6.8	9
75	MAGEMin, an Efficient Gibbs Energy Minimizer: Application to Igneous Systems. Geochemistry, Geophysics, Geosystems, 2022, 23, .	2.5	9
76	Coupled petrological-geodynamical modeling of a compositionally heterogeneous mantle plume. Tectonophysics, 2018, 723, 242-260.	2.2	8
77	Control of 3-D tectonic inheritance on fold-and-thrust belts: insights from 3-D numerical models and application to the Helvetic nappe system. Solid Earth, 2020, 11, 999-1026.	2.8	8
78	The hydraulic efficiency of single fractures: correcting the cubic law parameterization for self-affine surface roughness and fracture closure. Solid Earth, 2020, 11, 947-957.	2.8	8
79	Mountain Building in Taiwan: Insights From 3â€Ð Geodynamic Models. Journal of Geophysical Research: Solid Earth, 2019, 124, 5924-5950.	3.4	7
80	The Impact of a Very Weak and Thin Upper Asthenosphere on Subduction Motions. Geophysical Research Letters, 2019, 46, 11893-11905.	4.0	5
81	3D Geodynamic Models for HPâ€UHP Rock Exhumation in Oppositeâ€Dip Double Subductionâ€Collision Systems. Journal of Geophysical Research: Solid Earth, 2021, 126, e2021JB022326.	3.4	5
82	Comparison of continuous and discontinuous Galerkin approaches for variableâ€viscosity Stokes flow. ZAMM Zeitschrift Fur Angewandte Mathematik Und Mechanik, 2016, 96, 733-746.	1.6	4
83	An autonomous petrological database for geodynamic simulations of magmatic systems. Geophysical Journal International, 2020, 223, 1820-1836.	2.4	4
84	Recent advances in computational geodynamics: Theory, numerics and applications. Physics of the Earth and Planetary Interiors, 2008, 171, 2-6.	1.9	3
85	Heating glaciers from below. Nature Geoscience, 2013, 6, 683-684.	12.9	3
86	Quantification of Volcano Deformation Caused by Volatile Accumulation and Release. Geophysical Research Letters, 2022, 49, .	4.0	2
87	Constraining lithospheric flow. Science, 2016, 353, 1495-1496.	12.6	1
88	Geodynamic Modeling With Uncertain Initial Geometries. Geochemistry, Geophysics, Geosystems, 2022, 23, .	2.5	1
89	Simulating fluid injection in geological media with complex rheologies. IOP Conference Series: Earth and Environmental Science, 0, 249, 012005.	0.3	0